ACS OMEGA

http://pubs.acs.org/journal/acsodf

Article

Mechanism of the Aza-Piancatelli Reaction: Scope and Limitations of Furan Substitution in Donor−Acceptor Stenhouse Adduct Synthesis

Beatriz Peñín, Nil Sanosa, Diego Sampedro,* and Ignacio Funes-Ardoiz*

Cite This: *ACS Omega* 2022, 7, 22811−22817

Read Online

ACCESS | Metrics & More | Article Recommendations | Supporting Information

ABSTRACT: The aza-Piancatelli reaction has been widely used to synthesize donor−acceptor Stenhouse adducts (DASAs), a new class of molecular photoswitches with unique properties. However, the substitution pattern of furan cores has been limited to position 3, as 3,4-disubstituted furans remain unreactive. Herein, we explore the aza-Piancatelli reaction mechanism using density functional theory (DFT) calculations to understand the influence of the different substituents on the reactivity. We found that all the reaction pathways are kinetically accessible, but the driving force of the reaction is lost in disubstituted furans due to the loss of conjugation in the DASA products. Finally, a simple model is proposed to guide the design of synthetic routes using this reaction.

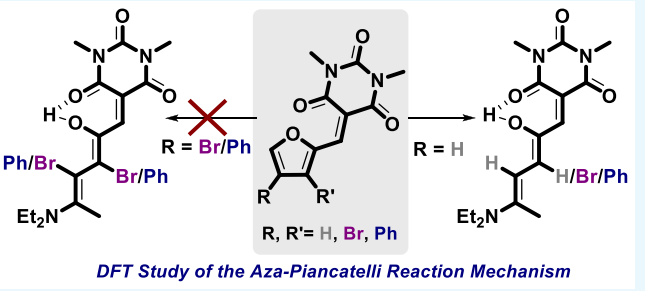

DFT Study of the Aza-Piancatelli Reaction Mechanism

INTRODUCTION

Donor−acceptor Stenhouse adducts (DASAs) are a new and promising class of photoswitches.[1] Although these compounds were first prepared in 2014,[2] they have already attracted considerable attention due to their unique features.[3] The DASA photoswitching mechanism is based on the light-activated equilibrium between a colored, open triene form and a colorless cyclic enone form. Then, the back-reaction is usually performed at room temperature (Scheme 1A). The negative photochromism of the process[4] together with the absorption in the visible and far-red region of the spectrum[5] and the large changes in the molecular structure and dipole moment of the two isomers have allowed their use in different applications.[6]

From a structural point of view, DASAs are a type of push−pull systems connected by a triene bridge. The different moieties used in both ends (donor and acceptor parts) have been modified in the last years to synthesize three different generations of compounds. These generations differ mainly in the solvent in which they can switch, the wavelength of absorption, and the stability of the closed form.[7] In turn, the structural modifications also cause some minor changes in the mechanism, although the general photoswitching mechanism is similar for all of them.[8] The isomerization mechanism in DASAs is considerably more complex than that of other classical photoswitches such as azobenzenes (simple *E*/*Z* isomerism), and it starts with a photochemical C=C isomerization followed by several thermal steps leading to cyclic isomer formation. The stability of these intermediates is affected by the donor and acceptor moieties, which justifies the changes in the properties upon substitution.

The control of the properties has been mainly introduced by the modification of the donor and acceptor moieties to prepare different generations of DASAs.[9] However, the triene π-bridge also has the potential to alter the thermal steps of the mechanism and modify some of the properties. This approach has been less explored for the change in the ends of the DASAs due to practical reasons. On one hand, the effect of substitution on the properties as a whole is hard to predict and may lead to improved optical properties (*i.e.*, red-shifted absorption) but poorer performance as a photoswitch.[10] On the other hand, the preparation of new DASAs with different substituents in the bridge has encountered synthetic problems. The key step for the synthesis of these compounds is usually based on the initial work by Šafář et al.,[11] where the opening of furan derivatives by amines leads to the open form of DASAs through the aza-Piancatelli reaction.[12] This reaction is based on the early work by the group led by Piancatelli, which originally reported the rearrangement of a 2-furylcarbinol into a 4-hydroxycyclopent-2-enone in acidic aqueous medium.[13] This first report was soon followed by a systematic study from the same group,[14] which set the ground for this very useful organic reaction. This transformation has been extensively used in the synthesis of natural products, partly due to its high level of stereocontrol, as the *trans* product is mainly formed.[15]

Received: April 19, 2022
Accepted: June 2, 2022
Published: June 16, 2022

Scheme 1. (A) Schematic Representation of DASAs as Photoswitches. (B) Synthesis of DASAs Using the Aza-Piancatelli Reaction[10]

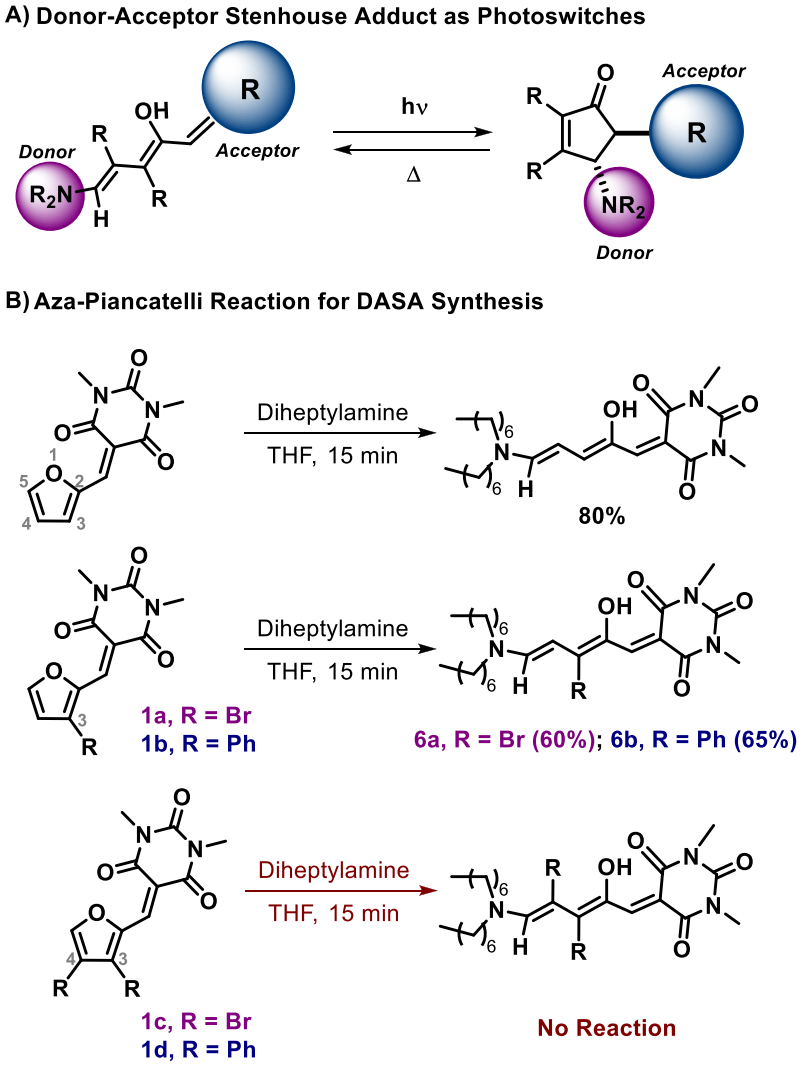

Recently, the aza version of the Piancatelli reaction has been used to prepare DASAs.[16] Substituents in the bridge of the resulting DASA come from the substituents in positions 3 and 4 in the furan moiety. We successfully synthesized[10] different DASAs through the opening of 3-substituted furans, but all our efforts to open 3,4-disubstituted furan rings were unsuccessful. However, exploration of this substitution pattern could contribute to the better understanding of the effects of these structural changes on the performance of these switches (Scheme 1B).

With these data in mind, we aimed to computationally evaluate the mechanism of the aza-Piancatelli reaction to understand the key aspects that prevent the reactivity of disubstituted furan rings and to extend the wide knowledge on the Piancatelli rearrangement mechanism.[17] This would complement the modular synthesis of DASAs, where both the donor and acceptor moieties can be easily varied but not the bridge position. Herein, we report the density functional theory (DFT) study on a series of five different furan rings, including the nonsubstituted one, the Ph and Br 3-substituted rings, and the Ph and Br 3,4- disubstituted ones.

RESULTS AND DISCUSSION

To initially explore the aza-Piancatelli mechanism, we chose the nonsubstituted furan ring as the first example (Scheme 2). Also, due to our experience in the synthesis of DASAs with barbituric acid as an acceptor and dialkyl amine as a donor (see Scheme 1), we used diethylamine as the nucleophile (to reduce the conformational space, compared to diheptylamine) and the corresponding derivative from furfural as the furan-ring reactant. The reaction starts with a weak hydrogen bonding interaction of the amine with adjacent oxygens from the furan ring and carbonyl groups, forming the weak adduct **2**, which is 7.2 kcal/mol higher in energy due to the loss of entropy. Then, the nucleophilic attack of the secondary amine is favored because of the strong conjugation along the delocalized sp^2 carbons of the furan and acceptor rings. The free energy barrier of this step is 20.2 kcal/mol ($\mathbf{TS}_{2\text{-}3}$), very accessible under reaction conditions, and the resulting species **3** is less stable than the initial adduct **2** due to the loss of aromaticity. Direct ring opening from this point is not possible, as the reaction barrier is very high, 59.0 kcal/mol ($\mathbf{TS}_{3\text{-}4'}$), because of the charge separation in the transition state, resulting in a nonstable ammonium-enol tautomer. In contrast, internal

https://doi.org/10.1021/acsomega.2c02439
ACS Omega 2022, 7, 22811−22817

Scheme 2. Computed Free Energy Profile of the Mechanism of the Aza-Piancatelli Reaction[a]

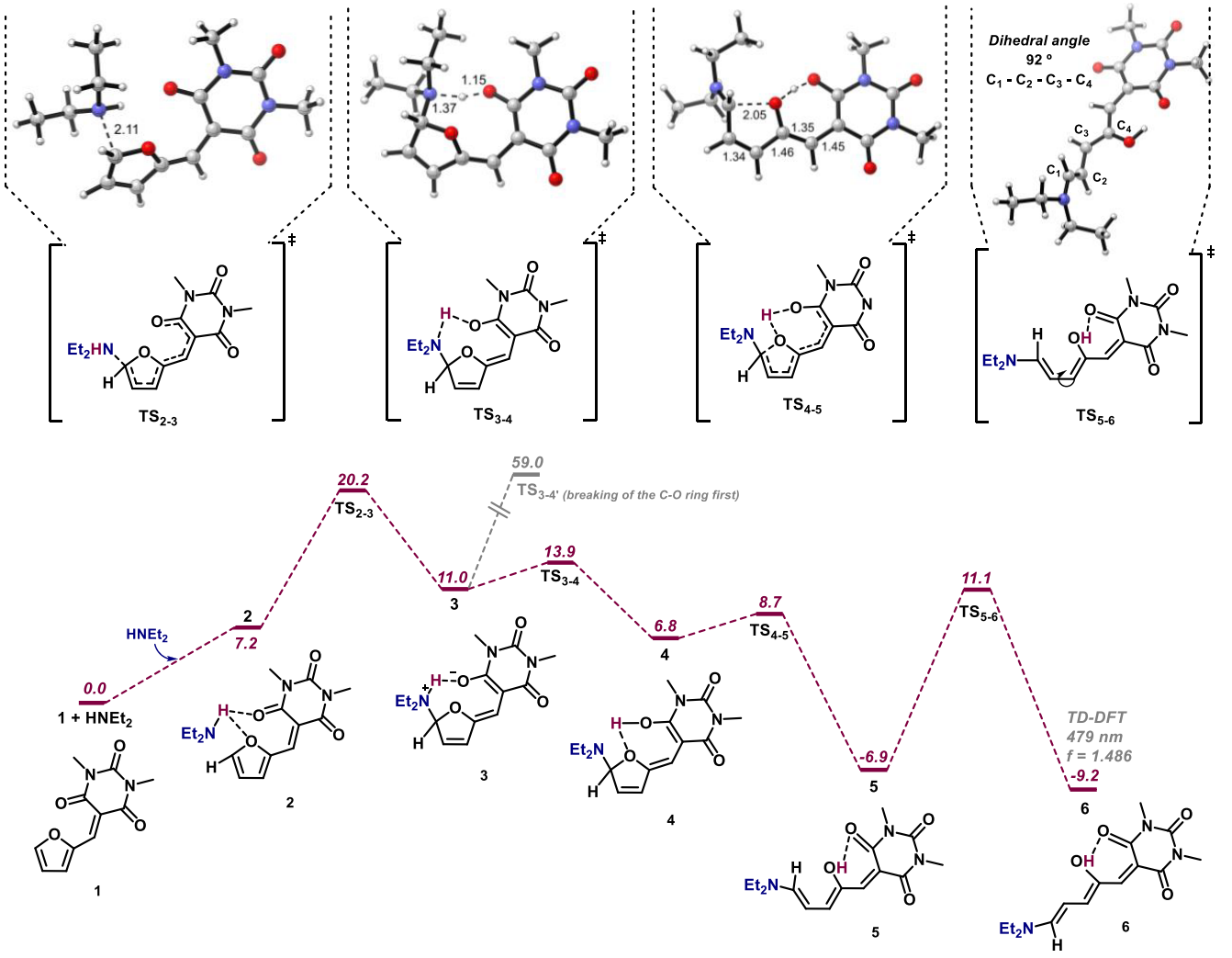

[a]Energies in kcal/mol.

proton transfer is almost barrierless through TS_{3-4}, forming intermediate **4** exergonically. This step starts with the proton transfer to the C═O in the barbituric acid, which finally forms a H-bond with the furan oxygen center in an asynchronous process. The explicit role of tetrahydrofuran (THF) in the proton transfer was not considered due to the low barrier observed, which might be even more favored in polar solvents such as THF. From this point, C-O bond breaking and proton transfer from OH in the barbituric acid to the furan O center are concerted and very favored through TS_{4-5} in an almost barrierless process (less than 2 kcal/mol) to form the *E*-enamine-conjugated *s-cis* product, which shows high stability even compared to that of the initial reactant (−6.9 kcal/mol). Finally, dihedral rotation of the intermediate **5** C−C bond occurs through a relatively high barrier, 18.0 kcal/mol, due to the large conjugation in the system, yielding the final *s-trans* product **6**. This donor−acceptor Stenhouse adduct exhibits a strong absorption, calculated at the time-dependent density functional theory (TD-DFT) level, at 479 nm (experimental λ_{max} = 570 nm in toluene),[2] associated with the cyclization reactivity as DASAs.

We then re-evaluated the mechanism in a set of six different mono- and disubstituted furan cores, using both Ph and Br as substituents (Scheme 3), due to our previous experience working with these compounds in the wet laboratory. According to the computed mechanisms, all the free energy profiles share a similar structure, where the initial three steps, from $\mathbf{1}^{R}$ to $\mathbf{5}^{R}$ (R = Br, Ph), are accessible in terms of kinetic barriers, with free energy barriers below 20 kcal/mol. Thus, even in disubstituted compounds, the nucleophilic attack event at TS_{1-2} is not affected by the proximity of the substituent, probably due to the out-of-the-plane attack. Then, the intramolecular proton transfer and the C−O bond breaking to open the ring are again very low in energy, with barriers generally below 5 kcal/mol.

However, we identified that there is an absence of stabilization in disubstituted compounds once the ring is opened. In these two pathways (Scheme 3, right), the *s-cis* isomer **5** is more stable than the *s-trans* and the accommodation of the substituents in both **5** and **6** in the plane is not possible, breaking the large conjugation along the carbon chain in the original monosubstituted DASAs due to the large steric hindrance (Scheme 4). These results indicate that the aza-Piancatelli reaction would be completely reversible for Ph- and Br-disubstituted compounds, and the isolation of the disubstituted DASA is not possible for these compounds,

https://doi.org/10.1021/acsomega.2c02439
ACS Omega 2022, 7, 22811−22817

Scheme 3. Comparison of the Free Energy Profiles of 3-substituted and 3,4-disubstituted Furan Rings (R = Br, Ph)[a,b]

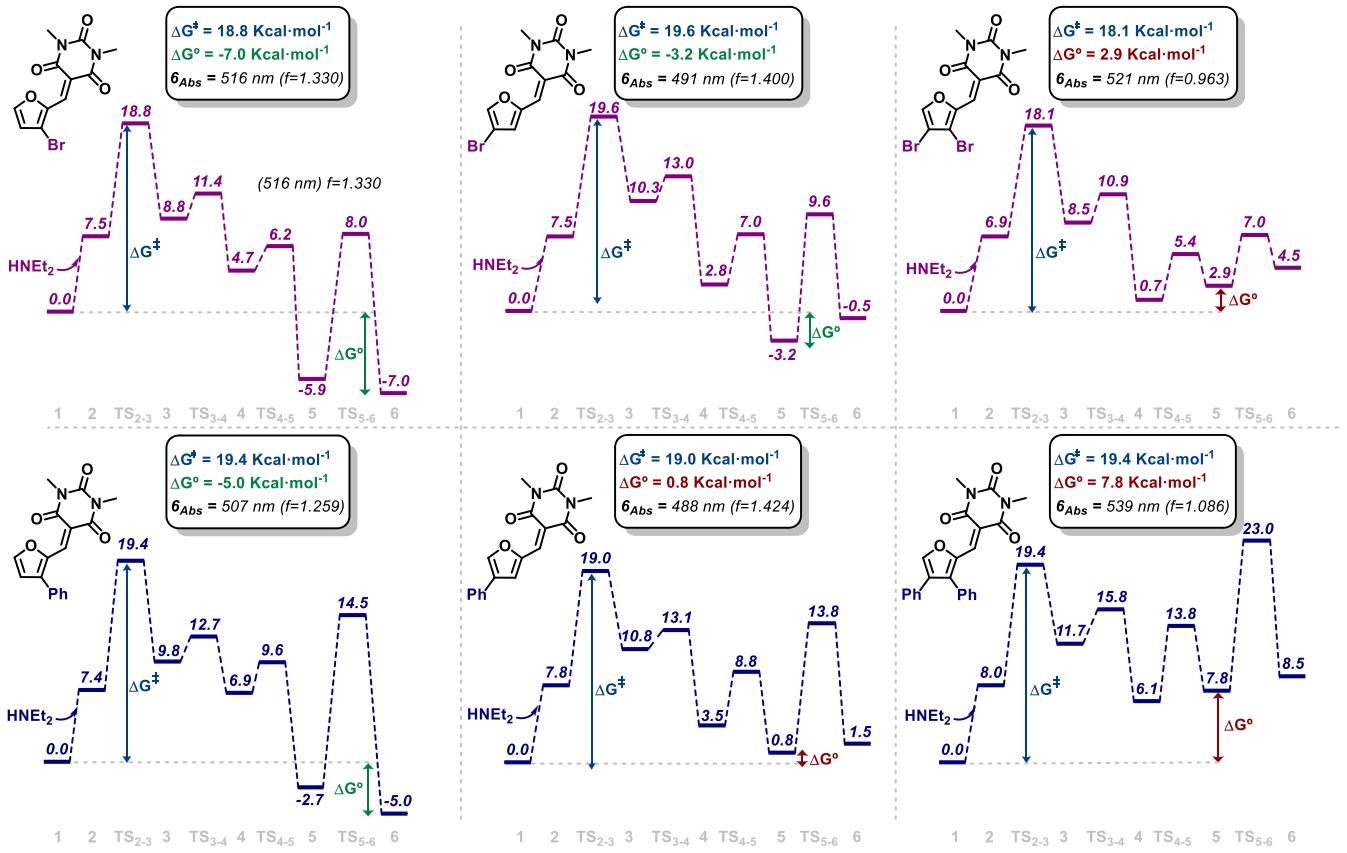

[a]The inset shows the highest free energy barrier of the profile and the overall thermodynamics of the process. [b]All energies in kcal/mol.

even considering other synthetic routes. In the case of monosubstituted compounds (Scheme 3, left and middle), the reaction mechanisms show the same pattern as for unsubstituted furan **1** in Scheme 2 for the 3-substituted furans, in agreement with the experimental observations of our previous synthetic trials. Also, 4-substituted furans were evaluated to analyze the effect of the substituent in this position. The overall computed thermodynamics place these compounds in between the 3-substituted and disubstituted furans, showing that the 4-position is more relevant to stability than the 3-position. However, the 4-bromide-substituted furan formation is exergonic and could be experimentally obtained. All the final compounds (**6**) share a strong absorption of light above 480 nm ($f \sim 1.00$), the disubstituted compound absorption being slightly red-shifted and weaker in intensity.

This mechanism shows that the aza-Piancatelli reaction is limited in terms of the thermodynamic driving force of the product formation and not in terms of kinetic accessibility. This allows us to rapidly explore substitution patterns computationally to identify a proper disubstituted candidate to be synthesized through this protocol. We have initially evaluated a series of substituents (Scheme 5) with different sizes and electronic properties. Again, most of the structures showed similar instability with respect to the starting material. Clearly, the ethyl chain is the least stable because it does not contribute to the overall conjugation of the molecule or add any new electrostatic interaction of hydrogen bonds. Also, the sp^3 character, compared to sp^2 substituents (ester, phenyl), exerts a detrimental effect on product formation, probably due to the larger steric hindrance. The influence of the electronic properties on the substituent is also very limited as the *p*-substituted cyanophenyl group is almost isoenergetic with respect to the unsubstituted phenyl substituent. Finally, we have identified that small-sized substituents, such as simple alkynyl groups, nitrile, and fluoride, can push forward the reactivity toward **5** and **6** and are therefore good candidates to try in the future.

CONCLUSIONS

In conclusion, we have computationally analyzed the mechanism of the aza-Piancatelli reaction by density functional theory calculations. The multistep mechanism starts with the nucleophilic attack of the amine, followed by an internal proton transfer and a ring-opening step through C−O bond breaking. The large conjugation of the resulting molecules serves as the driving force to compensate the breaking of the aromaticity of the initial furan ring. This is in fact true for nonsubstituted and disubstituted furan cores, but the weak conjugation of the disubstituted DASAs, due to the lack of accommodation of the substituents in the plane, prevents the formation of the molecular switch. Finally, with this data in hand, we propose a simple model based on the thermodynamic stability of the initial and final compounds to facilitate the election of substituents in synthetic routes. We hope this finding may help the community to rationally design new compounds, and further synthetic developments are still ongoing in our laboratory.

https://doi.org/10.1021/acsomega.2c02439
ACS Omega 2022, 7, 22811−22817

Scheme 4. Three-Dimensional (3D) Structure of Intermediates 5 and 6 in the Nonsubstituted and Bromide-Substituted Furans[a]

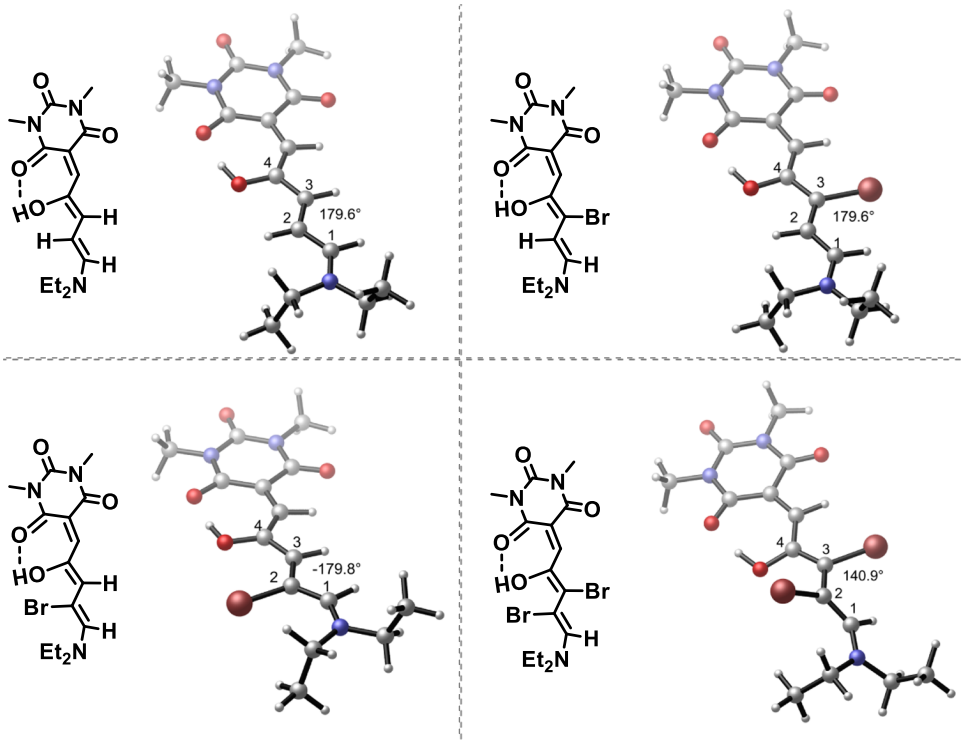

[a]The dihedral angle is shown in degrees.

Scheme 5. Exploration of Thermodynamic Stability of Intermediates 1, 4, and 5 in Disubstituted 3,4-Furan Cores[a]

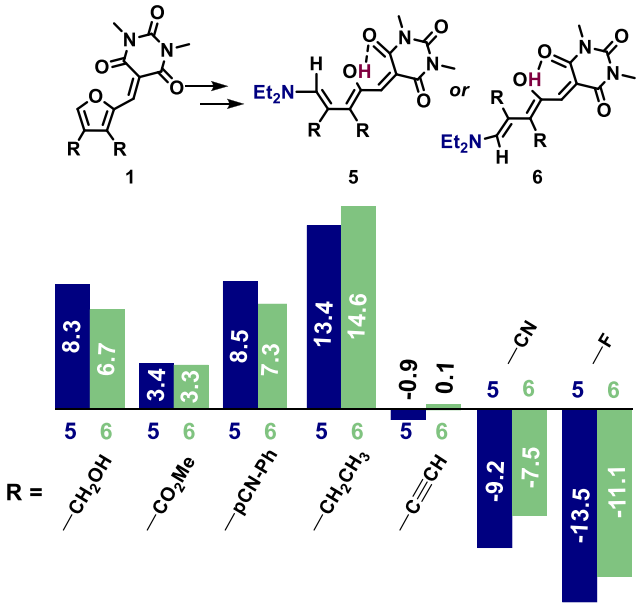

[a]Energies in kcal/mol referred to initial intermediate **1** + Et_2NH.

COMPUTATIONAL METHODS

Computational calculations were carried out using density functional theory and the Gaussian16 program package.[18] All the structures were optimized using the M06-2X functional,[19] which has been used and have good performance for pure organic systems,[20,21] in combination with the 6-31G(d) basis set. The nature of the stationary points was confirmed by frequency analysis, where minima have no imaginary frequencies and transition states have one imaginary frequency. Transition states were connected to the reactants and products by relaxing the active frequency and using IRC calculations when needed. In addition, all the potential energies were further refined by single-point calculations using the 6-311++G(d,p) larger basis set. Solvation was included using the SMD implicit solvation model[22] and THF as a solvent, which is used experimentally in the aza-Piancatelli reaction. The combination of M06-2X and SMD models has been demonstrated to be accurate for organic reactions in polar solvents.[23] 3D structures were prepared using the CYLview 1.0 program.[24]

ASSOCIATED CONTENT

Supporting Information

The Supporting Information is available free of charge at https://pubs.acs.org/doi/10.1021/acsomega.2c02439.

Cartesian coordinates and energies for all the calculated compounds (PDF)

Publication coordinates_final_revision (XYZ)

AUTHOR INFORMATION

Corresponding Authors

Diego Sampedro − *Departamento de Química, Centro de Investigación en Síntesis Química (CISQ), Universidad de La Rioja, 26006 Logroño, Spain;* orcid.org/0000-0003-2772-6453; Email: diego.sampedro@unirioja.es

Ignacio Funes-Ardoiz − *Departamento de Química, Centro de Investigación en Síntesis Química (CISQ), Universidad de La*

https://doi.org/10.1021/acsomega.2c02439
ACS Omega 2022, 7, 22811−22817

Rioja, 26006 Logroño, Spain; orcid.org/0000-0002-5843-9660; Email: ignacio.funesa@unirioja.es

Authors

Beatriz Peñín − *Departamento de Química, Centro de Investigación en Síntesis Química (CISQ), Universidad de La Rioja, 26006 Logroño, Spain*

Nil Sanosa − *Departamento de Química, Centro de Investigación en Síntesis Química (CISQ), Universidad de La Rioja, 26006 Logroño, Spain*

Complete contact information is available at: https://pubs.acs.org/10.1021/acsomega.2c02439

Notes

The authors declare no competing financial interest.

■ ACKNOWLEDGMENTS

We acknowledge the University of La Rioja for financial support. I.F.-A. thanks the "Ministerio de Ciencia e Innovación" for the Juan de la Cierva Incorporación scholarship (IJC2020-045125-I). We also thank the high-performance computing center of the University of La Rioja (Beronia) for computational resources.

■ REFERENCES

(1) (a) Browne, W.; Feringa, B. *Molecular Switches*; Wiley-VCH: Weinheim, 2011. (b) García-Iriepa, C.; Marazzi, M.; Frutos, L. M.; Sampedro, D. E/Z Photochemical switches: syntheses, properties and applications. *RSC Adv.* **2013**, *3*, 6241−6266.

(2) Helmy, S.; Leibfarth, F.; Oh, S.; Poelma, J.; Hawker, C. J.; de Alaniz, J. R. Photoswitching Using Visible Light: A New Class of Organic Photochromic Molecules. *J. Am. Chem. Soc.* **2014**, *136*, 8169−8172.

(3) Lerch, M. M.; Szymanski, W.; Feringa, B. L. The (photo)-chemistry of Stenhouse photoswitches: guiding principles and system design. *Chem. Soc. Rev.* **2018**, *47*, 1910−1937.

(4) Barachevsky, V. A. Negative photochromism in organic systems. *Rev. J. Chem.* **2017**, *7*, 334−371.

(5) García-Iriepa, C.; Marazzi, M. Level of Theory and Solvent Effects on DASA Absorption Properties Prediction: Comparing TD-DFT, CASPT2 and NEVPT2. *Materials* **2017**, *10*, No. 1025.

(6) Rifaie-Graham, O.; Ulrich, S.; Galensowske, N. F. B.; Balog, S.; Chami, M.; Rentsch, D.; Hemmer, J. R.; Read de Alaniz, J.; Boesel, L. F.; Bruns, N. Wavelength-Selective Light-Responsive DASA-Functionalized Polymersome Nanoreactors. *J. Am. Chem. Soc.* **2018**, *140*, 8027−8036.

(7) (a) Lerch, M. M.; Di Donato, M.; Laurent, A. D.; Medved, M.; Iagatti, A.; Bussotti, L.; Lapini, A.; Buma, W. J.; Foggi, P.; Szymanski, W.; Feringa, B. L. Solvent Effects on the Actinic Step of Donor−Acceptor Stenhouse Adduct Photoswitching. *Angew. Chem., Int. Ed.* **2018**, *57*, 8063−8068. (b) Hemmer, J. R.; Poelma, S. O.; Treat, N.; Page, Z. A.; Dolinski, N. D.; Diaz, Y. J.; Tomlinson, W.; Clark, K. D.; Hooper, J. P.; Hawker, C.; Read de Alaniz, J. Tunable Visible and Near Infrared Photoswitches. *J. Am. Chem. Soc.* **2016**, *138*, 13960−13966. (c) Hemmer, J. R.; Page, Z. A.; Clark, K. D.; Stricker, F.; Dolinski, N. D.; Hawker, C. J.; Read de Alaniz, J. Controlling Dark Equilibria and Enhancing Donor−Acceptor Stenhouse Adduct Photoswitching Properties through Carbon Acid Design. *J. Am. Chem. Soc.* **2018**, *140*, 10425−10429.

(8) (a) Di Donato, M.; Lerch, M. M.; Lapini, A.; Laurent, A. D.; Iagatti, A.; Bussotti, L.; Ihrig, S. P.; Medved, M.; Jacquemin, D.; Szymanski, W.; Buma, W. J.; Foggi, P.B.; Feringa, B. L. Shedding Light on the Photoisomerization Pathway of Donor−Acceptor Stenhouse Adducts. *J. Am. Chem. Soc.* **2017**, *139*, 15596−15599. (b) García-Iriepa, C.; Marazzi, M.; Sampedro, D. From Light Absorption to Cyclization: Structure and Solvent Effects in Donor-Acceptor Stenhouse Adducts. *ChemPhotoChem* **2019**, *3*, 866−873.

(9) Berraud-Pache, R.; Santamaría-Aranda, E.; de Souza, B.; Bistoni, G.; Neese, F.; Sampedro, D.; Izák, R. Redesigning donor−acceptor Stenhouse adduct photoswitches through a joint experimental and computational study. *Chem. Sci.* **2021**, *12*, 2916−2924.

(10) Martínez-López, D.; Santamaría-Aranda, E.; Marazzi, M.; Garcia-Iriepa, C.; Sampedro, D. π-Bridge Substitution in DASAs: The Subtle Equilibrium between Photochemical Improvements and Thermal Control. *Chem. - Eur. J.* **2021**, *27*, 4420−4429.

(11) Šafář, P.; Považaneca, F.; Prónayováb, N.; Baranc, P.; Kickelbickd, G.; Kožíšeke, J.; Brezaf, M. Dichotomy in the Ring Opening Reaction of 5-[(2-Furyl)methylidene]-2,2-dimethyl-1,3-dioxane-4,6-dione with Cyclic Secondary Amines. *Collect. Czech. Chem. Commun.* **2000**, *65*, 1911−1938.

(12) Piutti, C.; Quartieri, F. The Piancatelli Rearrangement: New Applications for an Intriguing Reaction. *Molecules* **2013**, *18*, 12290−12312.

(13) Piancatelli, G.; Scettri, A.; Barbadoro, S. A useful preparation of 4-Substituted-5-hydroxy-3-oxocyclopentene. *Tetrahedron Lett.* **1976**, *17*, 3555−3558.

(14) Piancatelli, G.; Scettri, A. Heterocyclic steroids-III: The synthetic utility of a 2-Furyl steroid. *Tetrahedron* **1977**, *33*, 69−72.

(15) Habermas, K. L.; Denmark, S. E.; Jones, T. K. The Nazarov Cyclization. In *Organic Reactions*, Paquette, L. A., Ed.; John Wiley & Sons, Inc.: New York, NY, 2004; Vol. *45*, pp 1−158.

(16) Veits, G. K.; Wenz, D. R.; Read de Alaniz, J. Versatile method for the synthesis of 4-Aminocyclopentenones: Dysprosium(III) triflate catalyzed aza-piancatelli rearrangement. *Angew. Chem., Int. Ed.* **2010**, *49*, 9484−9487.

(17) (a) Nieto Faza, O.; Silva López, C.; Alvarez, R.; de Lera, A. R. Theoretical Study of the Electrocyclic Ring Closure of Hydroxypentadienyl Cations. *Chem. - Eur. J.* **2004**, *10*, 4324−4233. (b) Davis, R. L.; Tantillo, D. J. Theoretical Studies on Pentadienyl Cation Electrocyclizations. *Curr. Org. Chem.* **2010**, *14*, 1561−1577.

(18) Frisch, M. J.; Trucks, G. W.; Schlegel, H. B.; Scuseria, G. E.; Robb, M. A.; Cheeseman, J. R.; Scalmani, G.; Barone, V.; Petersson, G. A.; Nakatsuji, H.; Li, X.; Caricato, M.; Marenich, A. V.; Bloino, J.; Janesko, B. G.; Gomperts, R.; Mennucci, B.; Hratchian, H. P.; Ortiz, J. V.; Izmaylov, A. F.; Sonnenberg, J. L.; Williams-Young, D.; Ding, F.; Lipparini, F.; Egidi, F.; Goings, J.; Peng, B.; Petrone, A.; Henderson, T.; Ranasinghe, D.; Zakrzewski, V. G.; Gao, J.; Rega, N.; Zheng, G.; Liang, W.; Hada, M.; Ehara, M.; Toyota, K.; Fukuda, R.; Hasegawa, J.; Ishida, M.; Nakajima, T.; Honda, Y.; Kitao, O.; Nakai, H.; Vreven, T.; Throssell, K.; Montgomery, J. A., Jr.; Peralta, J. E.; Ogliaro, F.; Bearpark, M. J.; Heyd, J. J.; Brothers, E. N.; Kudin, K. N.; Staroverov, V. N.; Keith, T. A.; Kobayashi, R.; Normand, J.; Raghavachari, K.; Rendell, A. P.; Burant, J. C.; Iyengar, S. S.; Tomasi, J.; Cossi, M.; Millam, J. M.; Klene, M.; Adamo, C.; Cammi, R.; Ochterski, J. W.; Martin, R. L.; Morokuma, K.; Farkas, O.; Foresman, J. B.; Fox, D. J.. *Gaussian 16*, Revision C.01; Gaussian, Inc.: Wallingford CT, 2016.

(19) Zhao, Y.; Truhlar, D. G. The M06 suite of density functionals for main group thermochemistry, thermochemical kinetics, noncovalent interactions, excited states, and transition elements: two new functionals and systematic testing of four M06-class functionals and 12 other functionals. *Theor. Chem. Acc.* **2008**, *120*, 215−241.

(20) Mardirossian, N.; Head-Gordon, M. Thirty years of density functional theory in computational chemistry: an overview and extensive assessment of 200 density functionals. *Mol. Phys.* **2017**, *115*, 2315−2372.

(21) Yu, P.; Chen, T. Q.; Yang, Z.; He, C. Q.; Patel, A.; Lam, Yu.-H.; Liu, C.-Y.; Houk, K. N. Mechanisms and Origins of Periselectivity of the Ambimodal [6 + 4] Cycloadditions of Tropone to Dimethylfulvene. *J. Am. Chem. Soc.* **2017**, *139*, 8251−8258.

(22) Marenich, A. V.; Cramer, C. J.; Truhlar, D. G. Universal solvation model based on solute electron density and a continuum model of the solvent defined by the bulk dielectric constant and atomic surface tensions. *J. Phys. Chem. B* **2009**, *113*, 6378−6396.

(23) (a) Mayer, R. J.; Allihn, P. W. A.; Hampel, N.; Mayer, P.; Sieber, S. A.; Ofial, A. R. Electrophilic reactivities of cyclic enones and α,β-unsaturated lactones. *Chem. Sci.* **2021**, *12*, 4850−4865. (b) Wang, J. Y. J.; Blyth, M. T.; Sherburn, M. S.; Coote, M. L. Tuning Photoenolization-Driven Cycloadditions Using Theory and Spectroscopy. *J. Am. Chem. Soc.* **2022**, *144*, 1023−1033.
(24) Legault, C. Y. *CYL View*, version 1.0 b; Université de Sherbrooke: http://www.cylview.org, 2009.

https://doi.org/10.1021/acsomega.2c02439
ACS Omega 2022, 7, 22811−22817